The Journal of Neuroscience, April 1989, 9(4): 1314–1324

Gating Scheme for Single GABA-Activated Cl^- Channels Determined from Stability Plots, Dwell-Time Distributions, and Adjacent-Interval Durations

David S. Weiss and Karl L. Magleby

Department of Physiology and Biophysics, University of Miami School of Medicine, Miami, Florida 33101

To study the gating of a GABA-activated Cl^- channel, currents from single channels activated by 1.0 μM GABA were examined in patches of membrane excised from cultured chick cerebral neurons. The distributions of open and shut interval durations were each described by the sum of 3 exponential components, suggesting that the channel normally enters at least 3 open and 3 shut states. Five different 6-state gating schemes were found that could describe, all equally well, the observed distributions of open and shut interval durations. Plots of the mean duration of open intervals adjacent to shut intervals of specified durations revealed that, on the average, openings of brief duration were adjacent to closings of long duration. This observation indicated 2 or more independent transition pathways between the open and shut states. Examination of the distributions of open intervals adjacent to shut intervals of specified durations revealed that the time constants of the exponential components describing these conditional open-interval distributions were independent of the durations of the adjacent shut intervals. In contrast, the areas changed in a manner consistent with open states of briefer mean lifetimes typically making transitions to shut states of longer mean lifetimes. Four of the 5 gating schemes considered were rejected because they did not predict the relationship between adjacent intervals or because they predicted that the channel should switch between 2 gating modes with markedly different mean open and shut times, which was not a characteristic of the experimental data. The single remaining kinetic scheme could account for the observed kinetic properties of the GABA channel.

GABA is the main inhibitory transmitter in the mammalian brain (Roberts, 1974; Enna and Gallagher, 1983), and a variety of clinically prescribed drugs, such as barbiturates and benzodiazepines, may exert some of their effects by modulating GABAergic transmission (Enna, 1981; Morselli and Lloyd, 1983). For these reasons, many studies have been directed at gaining a better understanding of the properties of the ion channels that underlie postsynaptic GABA responses (Barker et al., 1982; Jackson et al., 1982; Sakmann et al., 1983; Martin, 1985; Weiss, 1988; Weiss et al., 1988). Crucial to a better understanding of the properties and modulation of the GABA channel is detailed information on its steady-state gating behavior. The purpose of this study is to examine the kinetic properties of the Cl-selective GABA channel and determine which of a number of possible gating schemes best describes the observed steady-state channel activity.

Distributions of open and shut intervals were each described by the sum of 3 exponential components, suggesting at least 3 open and 3 shut states. Methods detailed by Colquhoun and Hawkes (1981) were then used to determine kinetic schemes consistent with the observed interval distributions. Five different 6-state gating schemes were found that described the distributions of open and shut intervals as well as theoretically possible. By examining the mean open and shut interval duration over time (to search for multiple kinetic modes) and the relationship between the durations of adjacent open and shut intervals, we were able to place additional constraints on the proposed gating scheme of the channel. Four of the 5 kinetic schemes were rejected because they were unable to predict both the observed inverse relationship between adjacent interval durations and the steady gating behavior of the channel. The single remaining scheme could account for the observed kinetic properties of the GABA channel. A preliminary report of these results has been presented in abstract form (Weiss et al., 1987).

Materials and Methods

Tissue culture. Experiments were performed on tissue-cultured chick cerebral neurons. Details of the culturing procedure are given in Thampy et al. (1983). Briefly, cerebral hemispheres were removed from stage-34 white Leghorn chicks and dissociated by extrusion through a 44-μm-pore nylon mesh into Dulbecco's modified Eagle's medium (DMEM). The cells (predominantly neuronal; Thampy et al., 1983) were then plated onto poly-L-lysine coated coverslips in 100 mm petri dishes containing DMEM plus 2% fetal calf serum and 8% donor calf serum. The cultures were maintained at 37°C in a 10% CO_2 environment, and recordings were made after 5–10 d.

Recording, sampling, and event detection. A coverslip containing the adhering neurons was placed in a chamber mounted to the stage of an Aus Jena microscope equipped with Hoffman modulation optics. The neurons were initially bathed in a saline consisting of (in mM): NaCl, 120; KCl, 5; glucose, 10; $MgCl_2$, 1; $CaCl_2$, 2; N-2-hydroxyethylpiperazine-N′-2-ethanesulphonic acid (HEPES)-NaOH, 10; pH, 7.4. Inside-out patches of membrane were obtained from the neurons using standard patch clamp techniques (Hamill et al., 1981).

As detailed in Weiss et al. (1988), GABA-gated Cl^- channels could be studied in isolation from other channel types when the patches of membrane were bathed in isotonic choline chloride. Recordings were made with the following saline in the patch pipette (in mM): choline

Received June 21, 1988; revised Sept. 2, 1988; accepted Sept. 9, 1988.

The experimental data were collected in the laboratory of John J. Hablitz on cultured neurons kindly supplied by Eugene M. Barnes, Jr. We thank Dr. David McCulloch for helpful discussions. This work was supported by an NIH fellowship (NS 08138) awarded to D.S.W. and grants from the NIH (AR 32805) and the Muscular Dystrophy Association to K.L.M.

Correspondence should be addressed to Dr. David S. Weiss, Department of Physiology and Biophysics (R-430), University of Miami School of Medicine, P.O. Box 016430, Miami, FL 33101.

chloride, 130; $CaCl_2$, 2; $MgCl_2$, 1; HEPES, 10; GABA (1 μM); pH, 7.4. After obtaining the inside-out patch, the intracellular face of the membrane was perfused using the method of Yellen (1982) with the following saline (in mM): choline chloride, 130; $MgCl_2$, 1; EGTA, 1; HEPES, 10; pH, 7.4. To avoid adding K^+ or Na^+ ions, the pH of all the above solutions was adjusted with tetraethylammonium hydroxide. Data were recorded with a Racal Store 4DS tape recorder.

Details of filtering, sampling, and event detection are in Weiss (1988). Briefly, the data were filtered at 0.8–1 kHz (−3 dB) and sampled every 80–140 μsec. The sampled data were then displayed for viewing. At this time any baseline drift could be adjusted and any clusters containing overlapping channels, if present, were discarded. Channel open and shut thresholds were set at 50% of the channel's open-current amplitude. Only threshold crossings with measured durations greater than the dead time of the system (180 or 225 μsec for 1 and 0.8 kHz, respectively) were counted. This had the effect of prolonging the mean open and shut interval durations owing to excluded brief events (Colquhoun and Sigworth, 1983; Blatz and Magleby, 1986a). All detected events were verified visually. The resulting open and shut interval durations were then stored in sequence in a file.

Stability plots. The stability of channel kinetics was assessed by examining the mean durations of open and shut intervals throughout the entire experiment. The first 50 open intervals and the first 50 shut intervals were each averaged separately. Then the next 50 open intervals and the next 50 shut intervals were averaged, and the process was repeated until the end of the file was reached. These mean values were then plotted against interval number. With these stability plots, any drift in the mean or switching between different kinetic modes (Blatz and Magleby, 1986b; McManus and Magleby, 1988) could be easily identified. Detailed analysis of channel kinetics was limited to periods over which the mean duration of both the open and shut intervals remained stable.

Binning and fitting distributions of open and shut intervals. All open and shut intervals were binned as the logarithm of their duration with 25 bins per log unit, as described in McManus et al. (1987). With this approach, the bin width increases for longer interval durations, but the relationship between bin width and bin midtime remains relatively constant. Such log-binning reduces the number of bins, thus speeding calculations and reducing random variation in the histograms (McManus et al., 1987). After binning the intervals, the maximum-likelihood method was used to determine the most likely values of the time constants and areas of the exponential components summing to describe the distributions (Colquhoun and Sigworth, 1983; McManus et al., 1987). The distributions were fitted starting at a time about twice the dead time to prevent the introduction of artifactual components (Roux and Sauve, 1985; Blatz and Magleby, 1986a). Starting with one exponential component, the number of components fitted to the data was increased one at a time until the improvement of the fit with the extra component was no longer significant ($p < 0.05$), as determined by the likelihood ratio test (Rao, 1973; Horn and Lange, 1983). The most likely number of exponential components was then the highest number which still gave a statistically significant improvement of the fit. For plotting, bins were often combined (with correction for bin width) to further reduce fluctuations.

Determining rate constants from the interval distributions. The following iterative technique was used to determine the most likely rate constants for a given kinetic scheme from the distributions of open and shut intervals (Blatz and Magleby, 1986a, b). Predicted open and shut probability density functions (PDF) were calculated for a given model and set of rate constants using a Q-matrix method (Colquhoun and Hawkes, 1981) with corrections for missed events due to filtering (Blatz and Magleby, 1986a). The likelihood that the experimentally observed data were drawn from this theoretical distribution was then calculated (Colquhoun and Sigworth, 1983), and the procedure was repeated with an iterative search routine until the rate constants were found that maximized the likelihood that the data were drawn from the open and shut interval distributions predicted by the examined kinetic scheme.

Relationship between adjacent open and shut times. The mean duration of open intervals adjacent to shut intervals of specified durations was determined by averaging all the open times immediately before and after shut intervals whose durations fell within the specified range. The specified shut ranges (usually 3) were selected so that they were well separated and had similar numbers of events. The mean of the adjacent open intervals was then plotted against the mean of all the shut intervals within that range. The mean duration of shut intervals adjacent to open intervals of specified durations was calculated and plotted in a similar manner.

In order to examine the distribution of open interval durations adjacent to shut intervals of a specified duration, the adjacent open intervals were binned and fit in the same manner as described in a previous section for the distribution of all the open intervals. The error bars for the time constants and areas describing these conditional distributions in Figure 5, *B, C,* represent the standard deviations obtained from 10 resamplings (Efron, 1982; Horn, 1987) of the adjacent intervals, which were then log-binned and fit with a sum of 3 exponential components. We favored this approach for assessing the expected range of the parameters because it also accounts, to some extent, for the stochastic variability in the distributions.

Determining the adjacent interval distributions and stability plots predicted by the different kinetic schemes. Simulation was used to predict, for a given scheme, stability plots and the means and distributions of open intervals adjacent to shut intervals of specified durations. To obtain the predicted result, intervals were first simulated for each kinetic scheme, taking into account the limited time resolution (Blatz and Magleby, 1986a, b; McManus et al., 1987), and then analyzed in the same manner as the experimental data.

Estimation of errors in determining rate constants for multichannel patches. Although the membrane patches analyzed in this study were selected so that only one channel appeared to be active at any one time, as indicated by steps to a single open current level during each cluster, it is likely that the patches contained more than one GABA channel. Since the time between clusters is determined mainly by the time required for any one of the inactive channels in the patch to become active, the mean duration of the shut intervals between clusters would be inversely related to the number of channels in a patch (Colquhoun and Hawkes, 1982).

Simulation was used to investigate errors that might arise from patches containing more than one channel. The assumption was made that data were obtained from membrane patches containing 1–3 GABA channels, each with the gating mechanism described by Scheme III (to be presented in the results). Idealized intervals for each channel were simulated (Blatz and Magleby, 1986a), filtered to give a dead time of 0.18 msec, and recorded separately on tape. Different random numbers were used in the simulation for each channel in the patch. The current records from 2 or 3 individual channels were then summed to simulate current from a multichannel patch. The combined data showed an occasional cluster with more than one active channel, as indicated by current steps to a second open level.

The generated current records for a patch containing 1, 2, or 3 channels were then sampled and analyzed to obtain estimates of the rate constants for Scheme III. Except for rate 6-5, the rates determined from the simulated data were typically within 5–20% of the rates used to generate the current records. Estimates of rate 6-5 increased almost directly with the number of channels in the patch. For example, in one simulation, the actual value of rate 6-5 used to generate data for each channel was 10.25 sec^{-1}. The value of rate 6-5 estimated from analysis of the simulated current record was 9.3 sec^{-1} for one channel in the patch, 19.2 sec^{-1} for 2 channels, and 26.1 sec^{-1} for 3 channels.

Thus, except for rate 6-5, reasonable estimates of the rates could be obtained from the simulated current records, even for patches containing up to 3 channels. Analysis of simulated data with more than 3 channels was not performed since the fraction of clusters with more than one active channel exceeded that observed in the experimental data. Estimated rates, in addition to rate 6-5, could be in error if data from such patches with many simultaneously active channels were analyzed.

Results

Appearance of GABA channel activity

Figure 1*A* shows currents recorded from GABA-activated Cl^- channels in the presence of 1 μM GABA. The channel openings (downward current steps) occur mainly in clusters. Figure 1*B* shows one such cluster of activity (from the region indicated by the bar in Fig. 1*A*) at a faster time resolution, and Figure 1*C* shows individual openings within this cluster (from the region indicated by the bar in Fig. 1*B*) at an even faster time resolution.

Each of the clusters most likely represents the activity of a single channel because there is a single open current level and

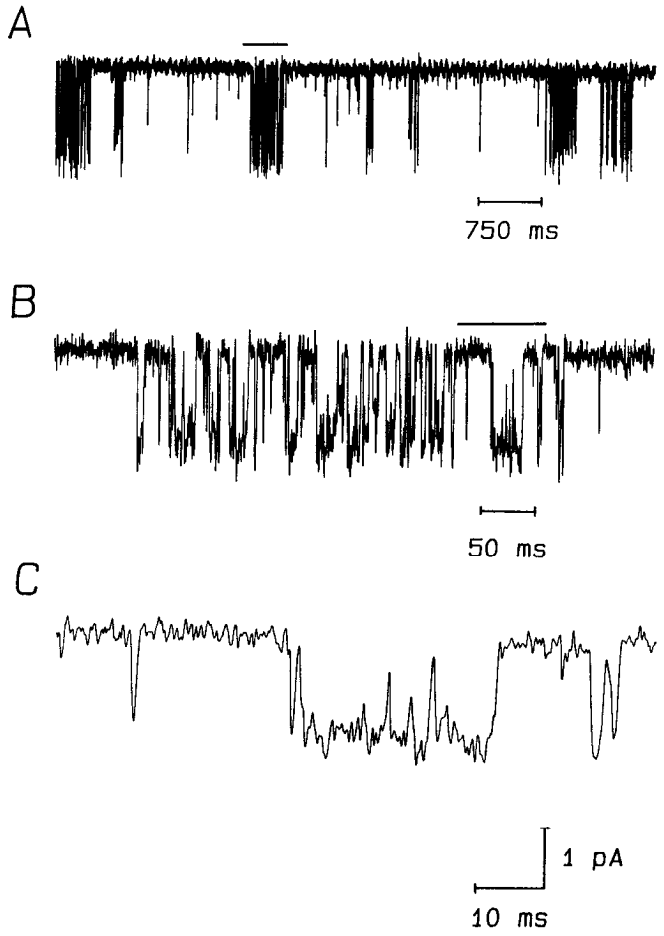

Figure 1. GABA-gated channel currents. Downward (inward) current indicates channel opening. *A,* Continuous record of channel activity showing openings grouped into clusters. Filtered at 240 Hz (−3 dB) for display. *B,* The cluster under the bar in *A* shown at higher time resolution. *C,* Activity under the bar in *B* shown at higher time resolution. Filtered at 0.8 kHz in *B* and *C*. Membrane potential, −60 mV.

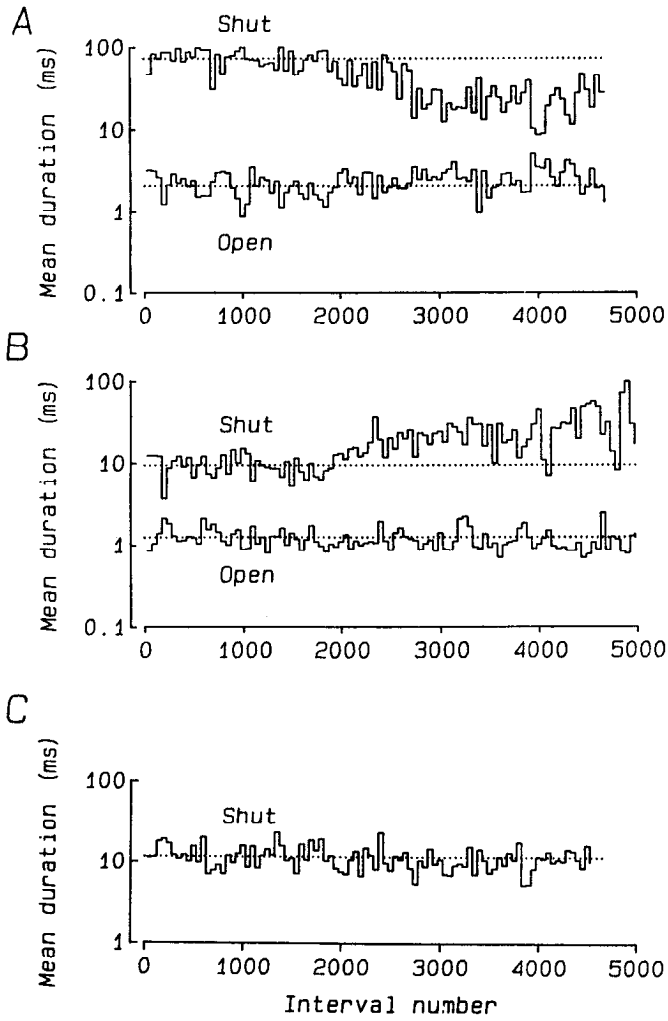

Figure 2. Stability plots of channel kinetics over time. Every 50 consecutive open and 50 consecutive shut intervals were averaged separately, and their mean was plotted against interval number. *A* and *B* present data for different channels. Only the first 1950 open intervals and 1950 shut intervals were analyzed further in *A,* and only the first 2000 open intervals and 2000 shut intervals were analyzed further in *B. C,* Stability plot of the shut intervals in *A* with all intervals with durations >50 msec excluded from the means but included in the interval number. Some means thus represent fewer than 50 intervals. *Dashed lines* are the average of the first 1950 intervals in *A,* the first 2000 intervals in *B,* and all the intervals in *C*. Membrane potential, −50 mV.

the clusters are well separated in time (Sakmann et al., 1980). All clusters, however, do not necessarily represent activity of the same GABA channel, because the number of channels in the patch is unknown. The data in this paper are from 4 patches in which the clusters are sufficiently separated, so that only 1 channel is typically active at any one time.

Assessment of channel stability

In order to assess the long-term stability of channel activity, the mean open and shut interval durations, determined from averages of every 50 consecutive open and 50 consecutive shut intervals, were plotted against the interval number (see Materials and Methods). The results for 2 patches, each with about 5000 open and 5000 shut intervals, are shown in Figure 2, *A, B.* The mean duration of the open intervals remained stable throughout the experiments, whereas the mean duration of the shut intervals began to decrease after the first 1950 intervals in Figure 2*A* and to increase after about 2000 intervals in Figure 2*B*.

These changes in the mean shut duration are likely to result from changes in the number of channels in the patch that are capable of being activated rather than from changes in the properties of individual channels. For instance, the increase in the mean shut duration in Figure 2*B* could reflect entry of one or more channels into desensitized or long-lived inactive states (Adams and Brown, 1975; Sakmann et al., 1980; Weiss, 1988), whereas the decrease in the mean shut duration in Figure 2*A* could reflect the return of one or more channels from such states. If this is true, then the mean shut interval duration within clusters should remain stable (since each cluster reflects the activity of a single channel) even when the overall mean shut interval is changing as a result of changes in the numbers of channels available for activation.

To test this possibility we ran stability plots with the long shut intervals (those greater than 50 msec in duration) excluded from the means. Results from the patch shown in Figure 2*A* are plotted in Figure 2*C*. Mean shut intervals within clusters remained constant throughout the experiment, suggesting stable

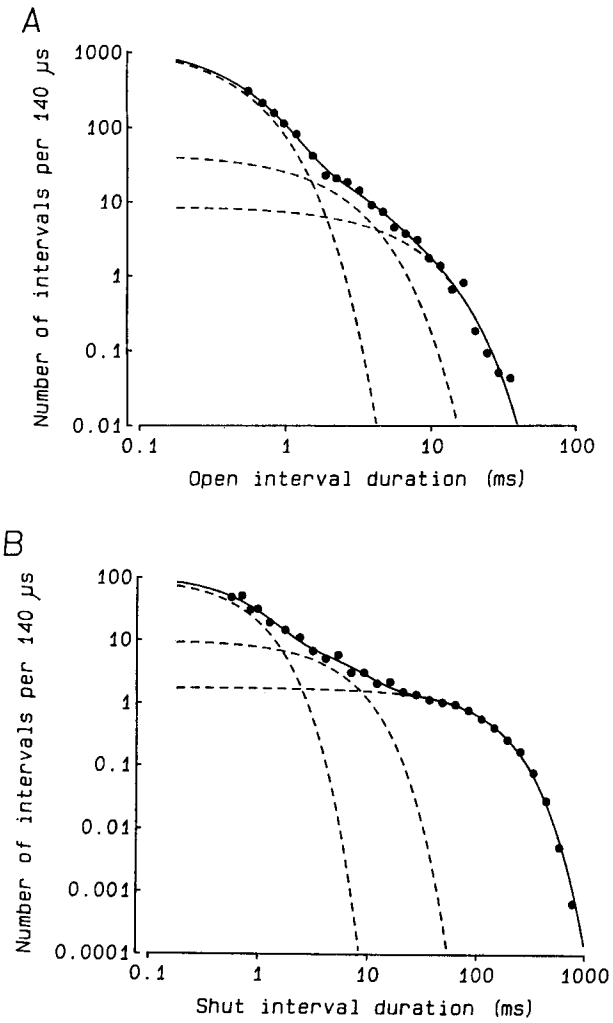

Figure 3. Distributions of all open and shut interval durations plotted on double logarithmic coordinates. *A,* Distribution of open intervals (*filled circles*) described by the sum of 3 exponential components (*continuous line*). *B,* Distribution of shut intervals (*filled circles*) described by the sum of 3 exponential components (*continuous line*). *Dashed lines* plot the individual components. Areas and time constants of the components are in Table 1.

kinetics once possible effects from changes in the number of channels capable of being activated are excluded. Also consistent with the possibility that the drift is due to a change in the number of channels capable of being activated is the observation that the mean open time remains stable as the mean shut time changes (Fig. 2, *A, B*); it has previously been shown that the open-channel kinetics of active GABA channels remain stable while the effective number of channels in a patch decreases due to desensitization (Weiss, 1988).

Independent of the mechanism for the drift of the mean shut interval durations in Figure 2, the stability plots reveal which segments of the data are sufficiently stable for further analysis. For example, the first 1950 open and 1950 shut intervals were selected for analysis in Figure 2*A*, and the first 2000 open and 2000 shut intervals were selected in Figure 2*B*. Although the results presented in this paper were verified with data from 4 different patches, all remaining figures are from the analysis of the first 1950 open and 1950 shut intervals in Figure 2*A*.

Table 1. Exponential components describing the distributions of open and shut times

Distribution	Components					
	Tau_1	$Area_1$	Tau_2	$Area_2$	Tau_3	$Area_3$
Open	0.36	0.77	1.83	0.14	5.87	0.09
Shut	0.62	0.21	4.82	0.16	105	0.63

Time constants (tau) in msec.

The GABA channel enters at least 3 open and 3 shut states

If the gating of GABA-activated channels results from transitions among discrete states, with the rates for transitions remaining constant in time, then each state will contribute an exponential component to the distribution of interval durations, although all components may not be detected experimentally (Colquhoun and Hawkes, 1981). In order to estimate the minimal number of open and shut states, histograms of open and shut times were constructed and the number of significant exponential components in the distributions was determined using maximum-likelihood fitting. Figure 3*A* plots the distribution of open times on double logarithmic coordinates, and Figure 3*B* presents a similar plot for shut times. Both distributions were best fit by the sum of 3 exponential components. The dashed lines plot the individual components, and the continuous lines plot their sum. Table 1 presents the time constants and areas of the components.

In all 4 patches examined, the open-interval distributions were best described by the sum of 3 exponential components. In 3 of the 4 patches the shut-interval distributions were best described by 3 components, with the remaining patch requiring 4 exponential components. These results suggest that the GABA channel typically enters at least 3 open and 3 shut states during normal activity.

Possible 6-state kinetic schemes

Given 3 open and 3 shut states, a variety of kinetic schemes can be constructed. The following schemes are 5 such possibilities, where C and O represent the closed and open states, respectively:

$$C_6 \leftrightarrow C_5 \leftrightarrow C_4 \leftrightarrow O_3 \leftrightarrow O_2 \leftrightarrow O_1 \quad \text{(I)}$$

$$\begin{array}{ccccccc} & & & & O_1 & & \\ & & & & \updownarrow & & \\ C_6 & \leftrightarrow & C_5 & \leftrightarrow & C_4 & \leftrightarrow & O_3 \\ & & & & \updownarrow & & \\ & & & & O_2 & & \end{array} \quad \text{(II)}$$

$$\begin{array}{ccccc} C_6 & \leftrightarrow & C_5 & \leftrightarrow & C_4 \\ & & \updownarrow & & \updownarrow \\ & & O_3 & & O_2 \leftrightarrow O_1 \end{array} \quad \text{(III)}$$

$$\begin{array}{ccccc} C_6 & \leftrightarrow & C_5 & \leftrightarrow & C_4 \\ \updownarrow & & \updownarrow & & \updownarrow \\ O_3 & & O_2 & & O_1 \end{array} \quad \text{(IV)}$$

$$\begin{array}{ccccc} C_6 & \leftrightarrow & C_5 & \leftrightarrow & C_4 \\ \updownarrow & & \updownarrow & & \updownarrow \\ O_3 & \leftrightarrow & O_2 & \leftrightarrow & O_1 \end{array} \quad \text{(V)}$$

For each of Schemes I–V and for all 4 data sets, a set of rate constants could be found that gave an excellent description of the distributions of open and shut interval durations. In fact, the distributions predicted by Schemes I–V were indistinguish-

able from the best fit sum of exponentials (continuous lines in Fig. 3). Since the best fit sum of exponentials gives the theoretical best fit for kinetic models with discrete states and with rate constants that remain fixed in time (discrete Markov model), then it follows that no models will be found that give a better description of the open and shut interval distributions than Schemes I–V. However, additional schemes might be found that give as good a description.

Thus, as discussed by Fredkin et al. (1985) and Bauer et al. (1987), an analysis restricted to the distributions of open and shut interval durations is not necessarily sufficient to distinguish among all possible gating schemes. Rather than expand the kinetic library by searching for additional schemes as likely as Schemes I–V, we have applied additional analysis techniques in order to distinguish the considered schemes.

The GABA channel has more than one gateway state

A fundamental difference between Schemes I and II and Schemes III–V is that in I and II all transitions between an open and shut state must pass through a single (gateway) shut state (C_4). Since all open states are adjacent to the same shut state, the durations of adjacent open and shut intervals should be independent (Colquhoun and Sakmann, 1985; Fredkin et al., 1985; Labarca et al., 1985; McManus et al., 1985; Colquhoun and Hawkes, 1987; Kerry et al., 1988). Schemes III–V, however, have more than 1 shut state from which the channel may open. Assuming that the mean lifetimes of the open states differ and the mean lifetimes of the shut states differ, then a dependent relationship between the durations of adjacent open and shut intervals is expected for Schemes III–V.

In order to investigate whether the kinetics of GABA-activated channels are consistent with gating schemes having single or multiple gateway states, we examined whether there was a dependent relationship between the durations of adjacent open and shut times. The shut intervals were divided into 3 groups with specified durations of 0–0.6 msec, 0.6–60 msec, and >60 msec. The mean duration of the open intervals adjacent to the shut intervals in each of the specified groups is then calculated from the experimental data and plotted as filled circles in Figure 4*A*. The mean duration of the adjacent open intervals decreases as the mean duration of the specified shut intervals increases. (The lines merely connect the points to show the trends in the data.) A similar inverse relationship was observed when the mean durations of shut intervals adjacent to open intervals with specified durations of 0–1.0 msec, 1.0–2.0 msec, and >2.0 msec were plotted (Fig. 4*B;* filled circles). These results demonstrate that, on average, the longer open intervals tend to be adjacent to the briefer shut intervals.

The predicted relationship of adjacent open and shut interval durations for Scheme I with its most likely rate constants was determined by simulation and plotted as open circles in Figure 4. Scheme I predicts, as expected for a model with a single gateway state, that adjacent open and shut interval durations are independent. A similar independent relationship was also found for Scheme II. Thus, Schemes I and II, as well as all other schemes with a single gateway state, may be excluded because they cannot account for the observed dependent relationship between adjacent interval durations.

Distributions of adjacent interval durations

Two possibilities which might account for the inverse relationship between adjacent open and shut times (Fig. 4) will be considered. In the first, the channel displays non-Markov gating kinetics, so that the rates for transitions among the open and shut states are not constant in time but depend upon preceding activity. If the opening and closing rates are inversely related to the durations of the dwell times in the preceding closed and open states, respectively, then an inverse relationship between open and shut interval durations could be observed. In the second possibility channel gating is Markovian such that the transition rates remain constant in time. If the kinetic scheme is constructed so that, in general, long open states are connected to brief shut states and brief open states are connected to long shut states, then an inverse relationship between adjacent open

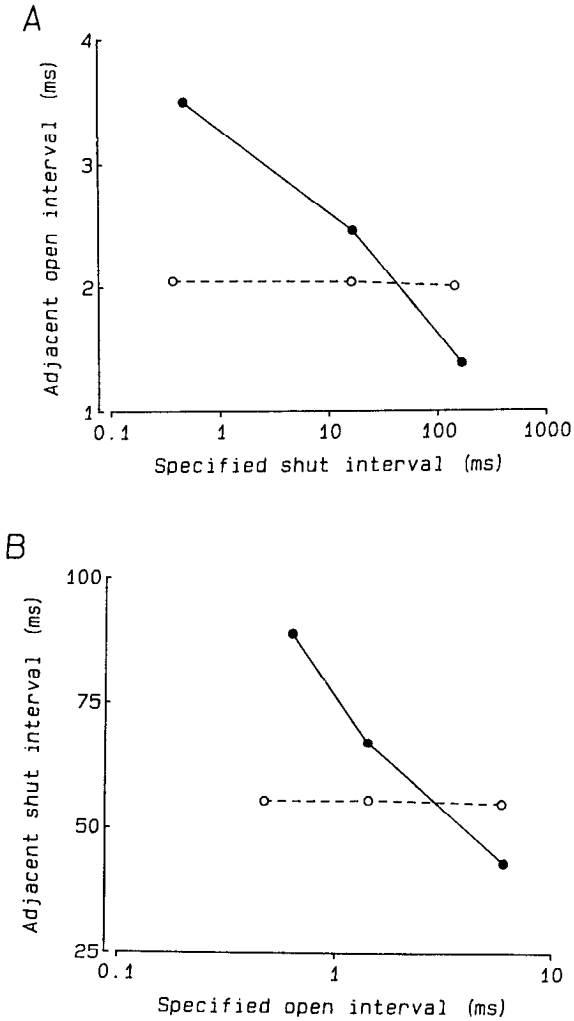

Figure 4. Inverse relationship between the mean durations of adjacent open and shut intervals. *A,* Plot of the mean durations of open intervals adjacent to shut intervals with specified durations of 0 to 0.6, 0.6 to 60, and >60 msec. The observed mean adjacent open interval duration is plotted against the mean duration of the shut intervals within each specified range (*filled circles*). Scheme I (*open circles*) predicts no dependence between adjacent interval durations. *B,* Plot of the mean durations of shut intervals adjacent to open intervals with specified durations of 0 to 1, 1 to 2, and >2 msec. The observed adjacent mean shut interval duration is plotted against the mean duration of the open intervals within each specified range (*filled circles*). Scheme I predicts no dependence between adjacent interval durations (*open circles*). Rate constants for Scheme I are (sec^{-1}): Rate 1-2, 249; rate 2-1, 97; rate 2-3, 459; rate 3-2, 447; rate 3-4, 18,163; rate 4-3, 9644; rate 4-5, 1102; rate 5-4, 177; rate 5-6, 141; rate 6-5, 48.

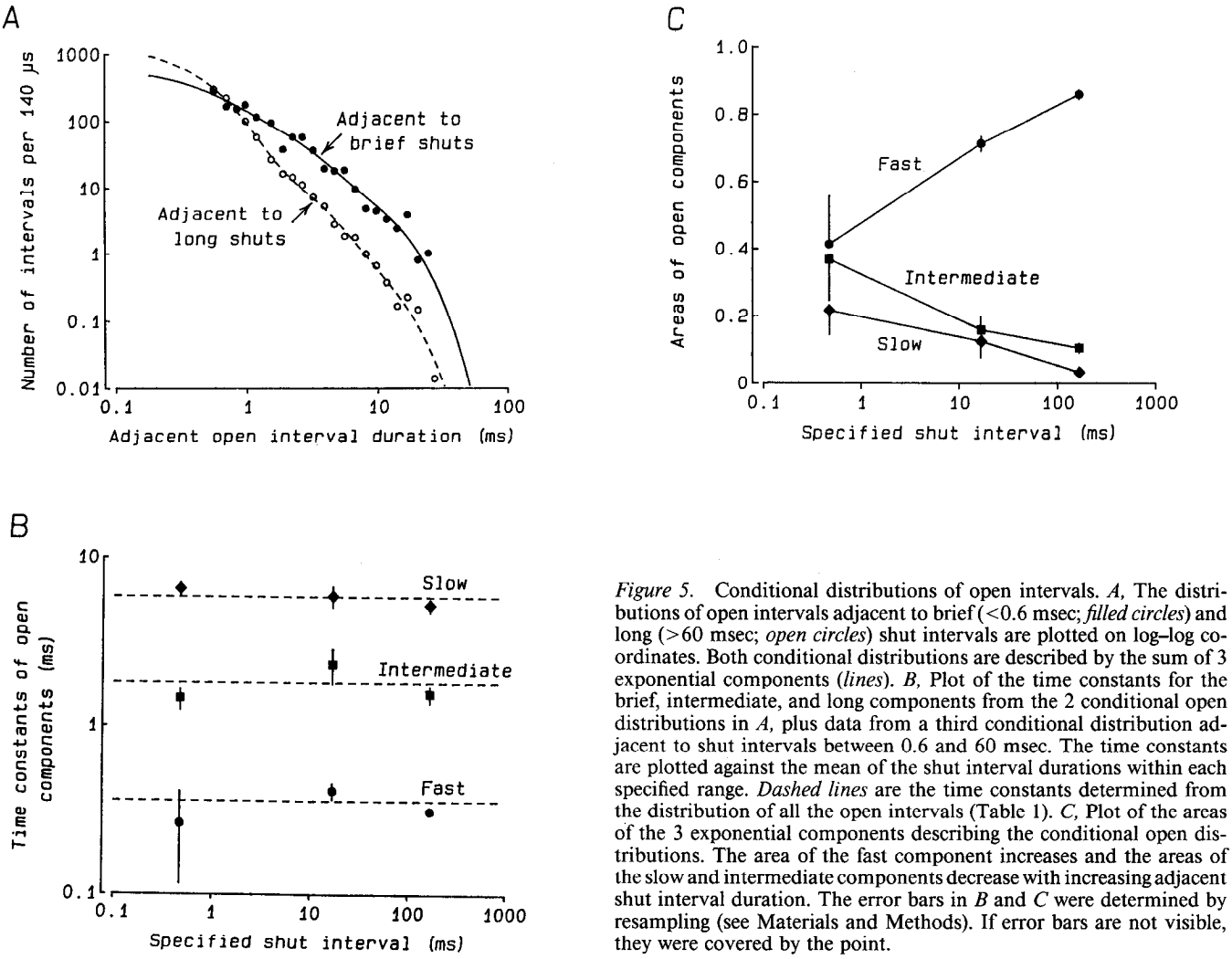

Figure 5. Conditional distributions of open intervals. *A,* The distributions of open intervals adjacent to brief (<0.6 msec; *filled circles*) and long (>60 msec; *open circles*) shut intervals are plotted on log–log coordinates. Both conditional distributions are described by the sum of 3 exponential components (*lines*). *B,* Plot of the time constants for the brief, intermediate, and long components from the 2 conditional open distributions in *A,* plus data from a third conditional distribution adjacent to shut intervals between 0.6 and 60 msec. The time constants are plotted against the mean of the shut interval durations within each specified range. *Dashed lines* are the time constants determined from the distribution of all the open intervals (Table 1). *C,* Plot of the areas of the 3 exponential components describing the conditional open distributions. The area of the fast component increases and the areas of the slow and intermediate components decrease with increasing adjacent shut interval duration. The error bars in *B* and *C* were determined by resampling (see Materials and Methods). If error bars are not visible, they were covered by the point.

and shut times could be observed. If the non-Markovian model is correct, then the time constants of the exponential components describing the distributions of open intervals adjacent to shut intervals of specified durations should depend on the duration of the specified shut intervals. If the Markovian model is correct, then the time constants of the exponential components should be independent of adjacent shut times (Fredkin et al., 1985), whereas the areas should be dependent on the adjacent shut times.

To distinguish between these 2 possibilities, we examined the distributions of open intervals adjacent to shut intervals of 3 specified ranges of durations (<0.6 msec, 0.6–60 msec, and >60 msec). The conditional open distributions adjacent to brief and long shut intervals are plotted on log–log coordinates in Figure 5*A*. The distributions are normalized to the same number of events for ease of comparison. The continuous and dashed lines plot the best fit sums of 3 exponential components to each conditional open distribution.

Figure 5*B* plots the time constants for the fast, intermediate, and slow components describing the 2 conditional open distributions (Fig. 5*A*) against the mean specified shut duration. Results from the conditional open distribution adjacent to shut intervals of intermediate durations are also presented. The time constant of each component in these conditional distributions is similar to the time constant of the corresponding component in the distribution of all the open intervals (dashed lines, values from Table 1). Time constants independent of the durations of adjacent intervals are consistent with Markov channel gating and inconsistent with the non-Markovian mechanism considered above.

Unlike the time constants, the areas of the components are dependent on the specified shut interval duration. The area of the fast component increases, and the areas of the intermediate and slow components decrease, as the adjacent mean shut duration increases (Fig. 5*C*). Thus, openings in the fast open component are more likely to occur adjacent to long shut intervals than to brief shut intervals, and openings from the slow and intermediate components are more likely to occur adjacent to brief shut intervals than to long shut intervals. These observations support the Markovian gating mechanism considered above in which the observed inverse relationship between the mean duration of adjacent open and shut intervals (Fig. 4) results from a change in the numbers of intervals forming each component, and not from a change in the time constants of the components.

Some schemes predict a modal gating behavior

For Schemes III–V we were able to find a set of rate constants for each scheme that described the distributions of all open and shut interval durations and generated an inverse relationship

Table 2. Rate constants for Scheme III from 4 patches

Rate	Patch number 1	2	3	4	Mean ± SD
1-2	231	299	164	171	216 ± 62.8
2-1	83.6	31.4	157	17.4	72.4 ± 63.2
2-4	486	620	734	652	623 ± 103
3-5	2810	4110	2270	1590	2695 ± 1067
4-2	1110	1210	1120	1010	1113 ± 81.8
4-5	609	971	951	597	782 ± 207
5-3	66.4	119	62.8	160	102 ± 46.4
5-4	13.0	119	36.9	44.3	53.3 ± 45.8
5-6	128	66.1	255	33.9	121 ± 97.6
6-5	41.1	17.3	102	71.3	57.9 ± 36.8

Rates are in sec^{-1}.

between adjacent interval durations. Schemes IV and V with their most likely rate constants, however, predicted behavior that was never observed in the experimental data. This is shown in Figure 6, in which the stability plots predicted by Scheme IV are presented (see figure legend for rate constants). Note how the mean open time (upper plot) switches between two markedly different values, in contrast to the experimental data shown in Figure 2. The mean shut time also demonstrates a coincident switching (lower plot). There are 2 modes because of the slow rate constants that separate C_4 and C_5, essentially uncoupling the 2 halves of the kinetic scheme. (Effects of uncoupling are discussed in Colquhoun and Hawkes, 1987.)

We were unable to find sets of rate constants for Schemes IV and V that predicted the distribution of open and shut interval durations and the inverse relationship between adjacent intervals while also predicting a non-modal gating behavior. Similar results were obtained in the 4 patches analyzed, and therefore Schemes IV and V are considered unlikely candidates for the GABA channel.

Scheme III describes all the experimental data

Scheme III is the only scheme for which a set of rate constants could be found which predicted all the experimental observations. The filled circles in Figure 7*A* plot the experimental distributions of all open and shut intervals. The distributions predicted by Scheme III (dashed lines) describe the data. The filled circles in Figure 7*B* plot the experimentally observed inverse relationship between adjacent open and shut times. Scheme III approximates the inverse relationship (open circles). Figure 7*C* plots the experimental distributions of open intervals adjacent to shut intervals of 2 specified ranges of durations (filled circles: <0.6 msec; open circles: >60 msec). Scheme III gave a reasonable description of these conditional open distributions (dashed and dotted lines). Figure 7*D* shows the stability plots predicted by Scheme III. The dotted lines are the means of the experimental data. As was true for the experimental data (Fig. 2), Scheme III predicted a single gating mode.

In all 4 patches examined, Scheme III gave the best description of the experimental data. Table 2 shows the rate constants derived for Scheme III for these 4 patches along with their means and standard deviations.

Discussion

In this study, single-channel recording methods and a quantitative analysis were used to obtain detailed information on the microscopic gating of a GABA-activated Cl^- channel. The result is a kinetic scheme which accounts for the observed kinetic properties of the channel.

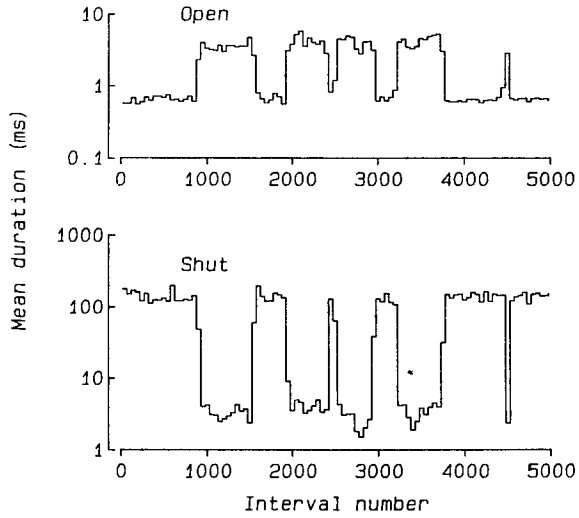

Figure 6. Stability plots predicted by Scheme IV with the indicated rates. The mean durations of both the open and the shut intervals (averaged 50 at a time) switched between 2 markedly different values. The rate constants for Scheme IV are (sec^{-1}): rate 1-4, 257; rate 4-1, 1773; rate 2-5, 687; rate 5-2, 242; rate 3-6, 2812; rate 6-3, 16; rate 4-5, 1.3; rate 5-4, 0.19; rate 5-6, 6.2; rate 6-5, 0.074.

The distributions of open and shut interval durations were each described by the sum of 3 exponential components, suggesting the GABA channel enters at least 3 open and 3 shut states. That there are 3 open states, compared to 2 found in a previous study (Weiss, 1988), probably reflects the greater sensitivity of maximum-likelihood methods in distinguishing exponential components. Multiple open and shut states are consistent with previous single-channel studies of the GABA channel that found evidence for 2 or more open states and 2 or more shut states (Sakmann et al., 1983; Bormann and Clapham, 1985; Martin, 1985; Rogers et al., 1987).

Five kinetic schemes with 3 open and 3 shut states were considered. Two of the 5 proposed schemes could be rejected because they were unable to predict the observed inverse relationship between the durations of adjacent open and shut intervals (Fig. 4). Two of the remaining 3 kinetic schemes were considered unlikely because, even though they were able to predict an inverse relationship between adjacent interval durations, they also predicted that the channel should switch between 2 different modes of behavior (Fig. 6), in contrast to the unimodal experimental data. Scheme III was the only scheme considered that predicted all the experimental observations (Fig. 7).

Limitations of the results

Other possible transition pathways and states. It cannot be ruled out that transition pathways and states in addition to those indicated in Schemes I–V may be involved in channel gating. For example, there may be a transition pathway between O_3 and O_2 in Scheme III. Such a pathway was not included because it did not improve the description of the distributions of interval durations in Figure 3. Lack of improvement, however, does not exclude that such a pathway is present. As pointed out by Bauer et al. (1987), the absence of a transition pathway in a kinetic scheme is equivalent to setting the rates for such a pathway to

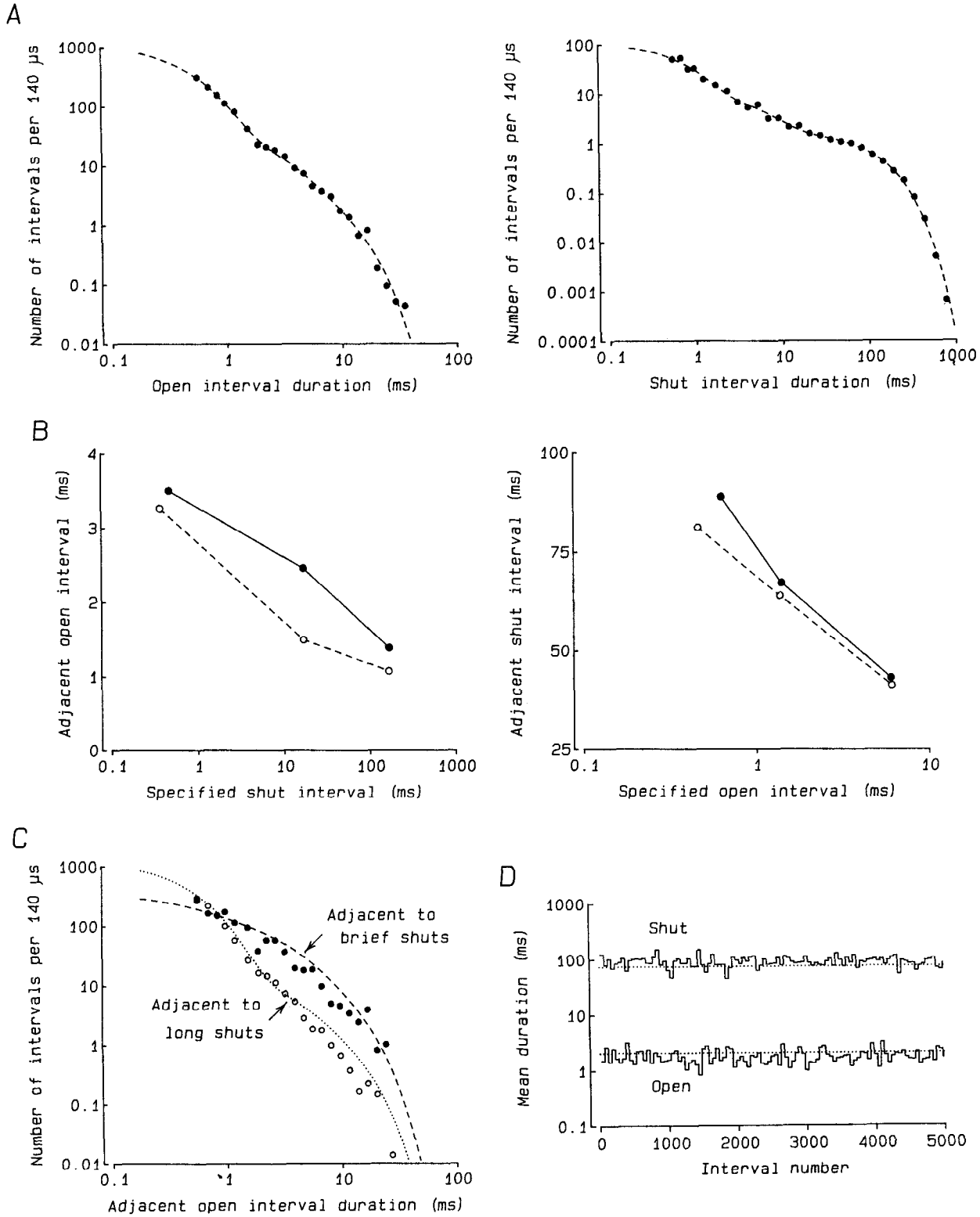

Figure 7. Scheme III accounts for the observed kinetic properties of the GABA channel. *A,* Observed (*filled circles*) and predicted (*dashed lines*) distributions of all open and shut interval durations. *B,* Observed (*filled circles*) and predicted (*open circles*) adjacent mean interval durations. Same specified durations as for Figure 4. *C,* Observed (*filled and open circles*) and predicted (*dashed and dotted lines*) conditional open distributions adjacent to brief (<0.6 msec) and long (>60 msec) shut intervals. *D,* Predicted stability plots. *Dotted lines* indicate the means of the observed open and shut interval durations. The rates used with Scheme III to calculate the predicted data are given in Table 2, patch 1.

zero. Thus, there is the implied assumption for Schemes I–V that the excluded transitions do not occur, but this assumption has not been tested directly. It is also possible that shut states of brief lifetime may be present, such as one between C_4 and O_1 in Scheme III, but were not detected due to the limited time resolution. However, Schemes I–V, with only the indicated states and transition pathways, did describe the open and shut interval distributions.

Uniqueness of the solutions. Although the information from the stability plots and adjacent interval plots was not directly utilized in the fitting procedure to derive the rate constants, this information was used to select sets of rate constants consistent with the observed data. Thus, it cannot be excluded that sets of rates might exist that would allow Schemes IV and V (which were rejected) to account for all the experimental data as well or better than Scheme III, although efforts to find such rates were unsuccessful. [Problems associated with determining whether unique solutions exist are discussed by Fredkin et al. (1985) and Bauer et al. (1987).] Independent of whether unique solutions exist for Schemes I and II, these schemes and all schemes containing a single gateway state can be rejected outright because they would be unable to account for the observed dependent relationship between the durations of adjacent intervals, whatever the rates (Colquhoun and Sakmann, 1985; Fredkin et al., 1985; McManus et al., 1985).

Binding steps not defined. Previous studies suggest that, on average, 2 molecules of GABA bind to the receptor to open the channel (Dichter, 1980; Sakmann et al., 1983; Akaike et al., 1985; Bormann and Clapham, 1985; Kaneko and Tachibana, 1986). The results of our study do not designate the 2 binding steps but account for the behavior of the channel in the presence of 1 μM GABA. Once the binding steps are identified, the concentration-dependent rates would assume units of $sec^{-1} \cdot \mu M^{-1}$.

More than one channel in a patch. The data analyzed for this study were selected so that only one channel appeared to be active at any one time, as indicated by steps to a single open current level during the clusters of activity (Fig. 1). Furthermore, since the open probability during the clusters was typically high, it is unlikely that more than one channel could have contributed to any cluster without detection. Nevertheless, the analyzed patches most likely contained more than one channel capable of being active, which can complicate the interpretation of the results. Some of the inactive GABA channels may be in a desensitized state owing to the prolonged exposure to GABA (Adams and Brown, 1975; Weiss et al., 1988); others may not be desensitized, but inactive because they are unliganded.

In analyzing the data, all shut intervals, including those which appeared to occur between clusters, were included in the distributions of shut intervals. This avoided the necessity of trying to distinguish between intervals occurring within and between clusters, as such a distinction is not possible for any single interval, except in terms of probability (Colquhoun and Hawkes, 1982). The consequence of including all intervals is that the component associated with the shut intervals between clusters of activity is included in the distributions and, consequently, this component contributes a shut state to the kinetic schemes. It is this component that is affected by the number of channels in the membrane patch.

Simulation indicated that reasonable estimates of all the rate constants should have been obtained from the experimental data, except for rate 6-5, which would increase approximately linearly with the number of channels in the patch (see Materials and Methods). The limitation on rate 6-5, however, would not interfere with the distinction among the schemes, because comparisons were always made separately for each patch. Thus the analysis, even with multichannel patches, was still sufficient to exclude all the considered gating mechanisms except Scheme III.

Scheme III with the rate constants (sec^{-1}) from patch 1 in Table 2 is:

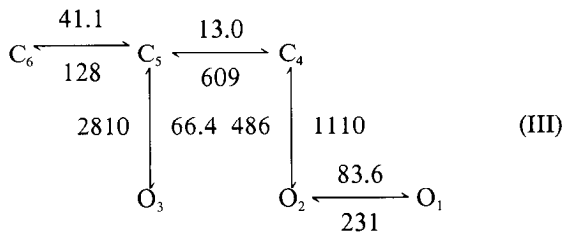

Scheme III presents a kinetic description of the observed data. Each C and each O represents a detected kinetic state, and the indicated rates represent the transition rates among the kinetic states. (Each kinetic state may represent more than one underlying conformational state, since conformational states with brief lifetimes or in rapid equilibrium with one another may not be detectable as separate kinetic states.) Since rate C_6–C_5 reflects the time required for one of the inactive channels in the patch to recover from desensitization and/or to bind agonist, rate C_6–C_5 is only an effective rate for the given membrane patch. In contrast to rate C_6–C_5, the other rates in Scheme III are those for a single active channel and would determine the activity during the clusters.

Kinetic interpretation of the proposed gating scheme

The mean lifetimes of the 6 states in Scheme III (calculated from 1/(sum of the rate constants leading away from that state) are (in msec): C_6, 24; C_5, 4.8; C_4, 0.58; O_3, 0.36; O_2, 1.8; O_1, 4.3. Starting in C_6, the channel will dwell an average of 24 msec before entering C_5. Once in C_5, the probability the channel will return to C_6 is 0.62, calculated from the rates as follows: 128/(128 + 66 + 13). Alternatively, the channel can open from C_5 to O_3 with a probability of 0.32, or make a transition to C_4 with a probability of 0.06. Because of the filtering and the brief lifetime of O_3, about 40% of the openings to O_3 are too brief to reach the half-amplitude criteria for detection. Some of these missed openings are apparent as brief events with reduced amplitude in Figure 1. Because so many of the transitions to O_3 are too brief to detect, it is the repeated transitions among C_6 and C_5 and the undetected transitions to O_3 that mainly give rise to the long component in the unconditional distribution of shut intervals (105 msec; Table 1). The long shut intervals usually terminate when an opening to O_3, the briefest open state, is detected. Thus, brief open intervals tend to be adjacent to long shut intervals (Figs. 1, 5*C*, 7*B*).

Once in C_4, the channel has a [1110/(1110 + 609)], or 0.65, chance of opening to the compound open state O_2–O_1, which gives rise to the intermediate and long open components. The brief shut component in the shut interval distribution arises mainly from sojourns to C_4, such as O_2–C_4–O_2 or O_1–O_2–C_4–O_2. Thus, intermediate and long open intervals tend to be adjacent to brief shut intervals (Figs. 1*C*, 5*C*, 7*B*).

Relation to other channel types

The amino acid sequence of the GABA receptor from bovine brain has been derived (Schofield et al., 1987). This sequence shows a remarkable homology to the amino acid sequence of the glycine receptor (Grenningloh et al., 1987) and the nicotinic acetylcholine receptor (Kubo et al., 1985). This has led to the proposal of a ligand-gated receptor superfamily (Barnard et al., 1987; Grenningloh et al., 1987; Schofield et al., 1987). The GABA and acetylcholine receptor share other properties as well. For instance, both receptors typically require 2 agonist molecules to open their channel (GABA: Dichter, 1980; Sakmann et al., 1983; Akaike et al., 1985; Bormann and Clapham, 1985; Kaneko and Tachibana, 1986; ACh: Dionne et al., 1978; Dreyer et al., 1978; Sakmann et al., 1985), both receptors inactivate (desensitize) with prolonged exposure to the agonist (GABA: Adams and Brown, 1975; ACh: Fatt, 1950; Katz and Thesleff, 1957), and both channels have 2 or more gateway states (GABA: this paper; ACh: Jackson et al., 1982; Colquhoun and Sakmann, 1985; Labarca et al., 1985).

Conclusion

Scheme III accounts for many of the kinetic properties of the GABA-activated chloride channel and should serve as a working hypothesis for further studies on gating, structure–function relationships, and investigations into the kinetic mechanism for the modulation of the channel by neuroactive drugs such as barbiturates and benzodiazapines.

References

Adams, P. R., and D. A. Brown (1975) Action of γ-aminobutyric acid on sympathetic ganglion cells. J. Physiol. (Lond.) *250:* 85–120.

Akaike, N., K. Hattori, N. Inomata, and Y. Oomura (1985) γ-Aminobutyric-acid- and pentobarbitone-gated chloride currents in internally perfused frog sensory neurones. J. Physiol. (Lond.) *360:* 367–386.

Barker, J. L., R. N. McBurney, and J. F. Macdonald (1982) Fluctuation analysis of neutral amino acid responses in cultured mouse spinal neurones. J. Physiol. (Lond.) *322:* 365–387.

Barnard, E. A., M. G. Darlison, and P. Seeburg (1987) Molecular biology of the $GABA_A$ receptor: The receptor/channel superfamily. Trends Neurosci. *10:* 502–509.

Bauer, R. J., B. F. Bowman, and J. L. Kenyon (1987) Theory of the kinetic analysis of patch-clamp data. Biophys. J. *52:* 961–978.

Blatz, A. L., and K. L. Magleby (1986a) Correcting single-channel data for missed events. Biophys. J. *49:* 967–980.

Blatz, A. L., and K. L. Magleby (1986b) Quantitative description of three modes of activity of fast chloride channels from rat skeletal muscle. J. Physiol. (Lond.) *378:* 141–174.

Bormann, J., and D. E. Clapham (1985) γ-Aminobutyric acid receptor channels in adrenal chromaffin cells: A patch-clamp study. Proc. Natl. Acad. Sci. USA *82:* 2168–2172.

Colquhoun, D., and A. G. Hawkes (1981) On the stochastic properties of single ion channels. Proc. R. Soc. Lond. [Biol.] *211:* 205–235.

Colquhoun, D., and A. G. Hawkes (1982) On the stochastic properties of bursts of single ion channel openings and of clusters of bursts. Proc. R. Soc. Lond [Biol.] *300:* 1–59.

Colquhoun, D., and A. G. Hawkes (1987) A note on correlations in single ion channel records. Proc. R. Soc. Lond. [Biol.] *230:* 15–52.

Colquhoun, D., and B. Sakmann (1985) Fast events in single-channel currents activated by acetylcholine and its analogues at the frog muscle end-plate. J. Physiol. (Lond.) *369:* 501–557.

Colquhoun, D., and F. J. Sigworth (1983) Fitting and statistical analysis of single-channel records. In *Single-Channel Recording,* B. Sakmann and E. Neher, eds., pp. 191–263, Plenum, New York.

Dichter, M. A. (1980) Physiological identification of GABA as the inhibitory transmitter for mammalian cortical neurons in cell culture. Brain Res. *190:* 111–121.

Dionne, V. E., J. H. Steinbach, and C. F. Stevens (1978) An analysis of the dose-response at voltage-clamped frog neuromuscular junctions. J. Physiol. (Lond.) *281:* 421–444.

Dreyer, F., K. Peper, and R. Sterz (1978) Determination of dose-response curves by quantitative ionophoresis at the frog neuromuscular junction. J. Physiol. (Lond.) *281:* 395–420.

Efron, B. (1982) *The Jackknife, the Bootstrap, and Other Resampling Plans,* Society for Industrial and Applied Mathematics, Philadelphia, PA.

Enna, S. J. (1981) Neuropharmacological and clinical aspects of γ-aminobutyric acid (GABA). In *Neuropharmacology of Central Nervous System and Behavioral Disorders,* G. Palmer, ed., pp. 507–537, Academic, New York.

Enna, S. J., and J. P. Gallagher (1983) Biochemical and electrophysiological characteristics of mammalian GABA receptors. Int. Rev. Neurobiol. *24:* 181–212.

Fatt, P. (1950) The electromotive action of acetylcholine at the motor end-plate. J. Physiol. (Lond.) *111:* 408–422.

Fredkin, D. R., M. Montal, and J. A. Rice (1985) Identification of aggregated Markovian models: Application to the nicotinic acetylcholine receptor. In *Proceedings of the Berkeley Conference in Honor of Jerry Neyman and Jack Kiefer,* Vol. 1, L. M. Le Cam, R. A. Olshen, and B. A. Belmont, eds., pp. 269–289, Wadsworth.

Grenningloh, G., A. Rienitz, B. Schmitt, C. Methfessel, M. Zensen, K. Beyreuther, E. D. Gundelfinger, and H. Betz (1987) The strychnine-binding subunit of the glycine receptor shows homology with nicotinic acetylcholine receptor. Nature *328:* 215–220.

Hamill, O. P., A. Marty, E. Neher, B. Sakmann, and F. J. Sigworth (1981) Improved patch-clamp techniques for high-resolution current recording from cells and cell-free membrane patches. Pfluegers Arch. *391:* 85–100.

Horn, R. (1987) Statistical methods for model discrimination: Applications to gating kinetics and permeation of the acetylcholine receptor channel. Biophys. J. *51:* 255–263.

Horn, R., and K. Lange (1983) Estimating kinetic constants from single channel data. Biophys. J. *43:* 207–223.

Jackson, M. B., H. Lecar, D. A. Mathers, and J. L. Barker (1982) Single channel currents activated by γ-aminobutyric acid, muscimol, and (−)-pentobarbital in cultured mouse spinal neurons. J. Neurosci. *2:* 889–894.

Jackson, M. B., B. S. Wong, C. E. Morris, H. Lecar, and C. Christian (1983) Successive openings of the same acetylcholine receptor channel are correlated in open time. Biophys. J. *42:* 109–114.

Kaneko, A., and M. Tachibana (1986) Effects of γ-aminobutyric acid on isolated cone photoreceptors of the turtle retina. J. Physiol (Lond.) *373:* 443–461.

Katz, B., and S. Thesleff (1957) A study of the 'desensitization' produced by acetylcholine at the motor end-plate. J. Physiol. (Lond.) *138:* 63–80.

Kerry, C. J., R. L. Ramsey, M. S. P. Sansom, and P. N. R. Usherwood (1988) Glutamate receptor channel kinetics: The effect of glutamate concentration. Biophys. J. *53:* 39–52.

Kubo, T., M. Noda, T. Takai, T. Tanabe, S. Kayano, S. Shimuzu, K. Tanaka, H. Takashi, T. Hirose, S. Inayama, R. Kikuno, T. Miyata, and S. Numa (1985) Primary structure of δ subunit precursor of calf muscle acetylcholine receptor deduced from cDNA sequence. Eur. J. Biochem. *149:* 5–13.

Labarca, P., J. A. Rice, D. R. Fredkin, and M. Montal (1985) Kinetic analysis of channel gating: Application to the cholinergic receptor channel and the chloride channel from *Torpedo californica.* Biophys. J. *47:* 469–478.

Martin, R. J. (1985) γ-Aminobutyric acid- and piperazine-activated single-channel currents from *Ascaris suum* body muscle. Br. J. Pharmacol. *84:* 445–461.

McManus, O. B., and K. L. Magleby (1988) Kinetic states and modes of single large-conductance calcium-activated potassium channels in cultured rat skeletal muscle. J. Physiol. (Lond.) *402:* 79–120.

McManus, O. B., A. L. Blatz, and K. L. Magleby (1985) Inverse relationship of the durations of adjacent open and shut intervals for Cl and K channels. Nature *317:* 625–627.

McManus, O. B., A. L. Blatz, and K. L. Magleby (1987) Sampling, log binning, fitting, and plotting durations of open and shut intervals from single channels and the effects of noise. Pfluegers Arch. *410:* 530–553.

Morselli, P. L., and K. G. Lloyd (1983) Clinical pharmacology of

GABA agonists. In *The GABA Receptors,* S. J. Enna, ed., pp. 305–336, Humana, Clifton, NJ.

Rao, C. R. (1973) *Linear Statistical Inference and its Applications,* Wiley, New York.

Roberts, E. (1974) Disinhibition as an organizing principle in the nervous system—The role of γ-aminobutyric acid. Adv. Neurol. *5:* 127–143.

Rogers, C. J., R. E. Twyman, and R. L. Macdonald (1987) GABA-activated chloride currents have multi-state kinetics in cultured murine spinal cord neurons. Soc. Neurosci. Abstr. *13:* 264.6.

Roux, B., and R. Sauve (1985) A general solution to the time interval omission problem applied to single channel analysis. Biophys. J. *48:* 149–158.

Sakmann, B., J. Patlak, and E. Neher (1980) Single acetylcholine-activated channels show burst kinetics in presence of desensitizing concentrations of agonist. Nature *286:* 71–73.

Sakmann, B., O. P. Hamill, and J. Bormann (1983) Patch-clamp measurements of elementary chloride currents activated by the putative inhibitory transmitters GABA and glycine in mammalian spinal neurons. J. Neural Trans. [Suppl.] *18:* 83–95.

Sakmann, B., C. Methfessel, M. Mishina, T. Takahashi, T. Takai, M. Kurasaki, K. Fukuda, and S. Numa (1985) Role of acetylcholine receptor subunits in gating of the channel. Nature *318:* 538–543.

Schofield, P. R., M. G. Darlison, N. Fujita, D. R. Burt, F. A. Stephenson, H. Rodriguez, L. M. Rhee, J. Ramachandran, V. Reale, T. A. Glencorse, P. H. Seeburg, and E. A. Barnard (1987) Sequence and functional expression of the $GABA_A$ receptor shows a ligand-gated receptor super-family. Nature *328:* 221–227.

Thampy, K. G., C. D. Sauls, B. R. Brinkley, and E. M. Barnes (1983) Neurons from chick embryo cerebrum: Ultrastructural and biochemical development *in vitro.* Dev. Brain Res. *8:* 101–110.

Weiss, D. S. (1988) Membrane potential modulates the activation of GABA-gated channels. J. Neurophysiol. *59:* 514–527.

Weiss, D. S., J. J. Hablitz, and K. L. Magleby (1987) Kinetic scheme for GABA-activated channels in cultured chick neurons. Neurosci. Abstr. *13:* 98a.

Weiss, D. S., E. M. Barnes, and J. J. Hablitz (1988) Whole-cell and single-channel recordings of GABA-gated currents in cultured chick cerebral neurons. J. Neurophysiol. *59:* 495–513.

Yellen, G. (1982) Single Ca-activated non-selective cation channels ion neuroblastoma. Nature *296:* 357–359.